Chinese Journal of Catalysis 34 (2013) 1267–1273 催化学报 2013年 第34卷 第6期 | www.chxb.cn

available at www.sciencedirect.com

ScienceDirect

journal homepage: www.elsevier.com/locate/chnjc

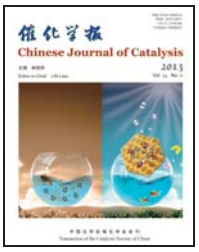

Article

Synthesis and characterization of P-doped TiO_2 thin-films for photocatalytic degradation of butyl benzyl phthalate under visible-light irradiation

R. M. MOHAMED [a,b,*], E. AAZAM [a]

[a] *Chemistry Department, Faculty of Science, King Abdulaziz University, P.O. Box: 80203, Jeddah 21589, Saudi Arabia*
[b] *Advanced Materials Department, Central Metallurgical R&D Institute, CMRDI, P.O. Box 87, Helwan, Cairo, Egypt*

ARTICLE INFO

Article history:
Received 21 January 2013
Accepted 4 March 2013
Published 20 June 2013

Keywords:
Phosphorus-doped
Titania
Thin film
Visible light
Photocatalyst

ABSTRACT

P-doped TiO_2 (PTIO) thin-films with different P contents were prepared using a sol-gel method. The thin-film samples were characterized using various techniques. The photocatalytic activity was evaluated by decomposing butyl benzyl phthalate under visible-light irradiation. The results showed that the transformation of anatase to the rutile phase was inhibited and grain growth of TiO_2 was prevented by P doping. The results confirm that the doped P atoms existed in two chemical forms, and those incorporated in the TiO_2 lattice may play a positive role in photocatalysis. The high photocatalytic activities of the PTIO thin-films may be the result of extrinsic absorption through the creation of oxygen vacancies, rather than excitation of the intrinsic absorption band of bulk TiO_2. The PTIO can be recycled with little depression of the photocatalytic activity. After six cycles, the photocatalytic activity of the PTIO film was still higher than 98%.

1. Introduction

Phthalate esters (PAEs) are the most abundant synthetic industrial chemicals. They are produced in large quantities and are mainly used as plasticizers in the manufacture of various plastics. The release of PAEs into the environment or wastewater effluents causes pollution and harm to human health. Some PAEs have been designated as priority organic pollutants by the United States Environmental Protection Agency and by regulatory authorities in some European countries, because they are ecologically toxic and hazardous [1]. However, PAEs in waterworks cannot be effectively removed using conventional water-treatment processes such as coagulation, sedimentation, filtration, and disinfection because of their refractory biodegradability and low photodegradability [2]. Effective treatments for these pollutants are therefore urgently needed. Photocatalytic processes have received considerable attention because of the efficiency of their mineralization, ideally producing carbon dioxide, water, and inorganic mineral ions as the end products. Recently, a small number of investigations of the degradation of PAEs under irradiation with ultraviolet (UV) light or sunlight, using semiconductors as photocatalysts, have been reported [3–7]. Nanocrystalline TiO_2 is a very attractive photocatalyst because of its high oxidative power, photostability, low cost, and nontoxicity. However, the large band gap of TiO_2 (3.2 eV) restricts its photocatalytic applications in the UV range. UV light accounts for merely 4% of the solar spectrum and can be readily filtered out, even by clear glass or pure water. Improving the optical properties of TiO_2 by modifying its band gap is therefore necessary. In recent decades, a number of studies of nonmetal doping have been conducted to shift the optical response of catalytically active TiO_2

* Corresponding author. Tel: +966-540715648 ; Fax: +966-2-6952292; E-mail: redama123@yahoo.com
DOI: 10.1016/S1872-2067(12)60572-5 | http://www.sciencedirect.com/science/journal/18722067 | Chin. J. Catal., Vol. 34, No. 6, June 2013

from the UV- to the visible-light region. Nitrogen [8–10], carbon [11,12], boron [13,14], sulfur [15,16], and phosphorus [17] have been introduced into the TiO_2 matrix to extend its photoresponsive range. Another drawback to the use of TiO_2 as a commercial photocatalyst is the need for a difficult and costly filtration step to eliminate nanoparticles and recycle the catalyst. The aim of the current work is therefore the preparation and characterization of P-doped TiO_2 (PTIO) thin-films via a sol-gel method, to overcome the problem of separation of the photocatalyst by thin-film preparation, and to use P doping to shift the TiO_2 absorption from the UV region to the visible region. The photocatalytic performances of the PTIO thin-film photocatalysts were evaluated through the degradation of butyl benzyl phthalate (BBP) under visible-light irradiation.

2. Experimental

2.1. Photocatalyst preparation

Titanium tetrabutyl titanate $Ti(OBu)_4$ was chosen as the Ti precursor. Hypophosphorous acid was used as the P source for the PTIO samples. Hypophosphorous acid was added to distilled water under vigorous stirring. A mixture of $Ti(OBu)_4$ and propanol was added dropwise to the water, the pH of which was adjusted to 2.0 with nitric acid, until the $Ti(OBu)_4$ was completely hydrolyzed. The molar ratios of P and Ti were 1:100; 2:100; 3:100, and 4:100. The solution was refluxed at 80 °C for 24 h to obtain a PTIO sol. Pure TiO_2 (TIO) samples were prepared by the same method, but without adding hypophosphorous acid. Glass plates, 60 mm × 20 mm, used as substrates, were dipped in the obtained PTIO and TIO sols for 30 min, dried in a vacuum oven at 60 °C for 2 h, and then cooled in the atmosphere. The produced thin-film samples were denoted by TIO, PTIO-0.01, PTIO-0.02, PTIO-0.03, and PTIO-0.04. We used TiO_2 Degussa (P_{25}) as a reference photocatalyst for comparisons of catalytic activities.

2.2. Photocatalyst characterization

The specific surface areas of the prepared samples were evaluated using nitrogen adsorption-desorption isotherms at −196 °C, measured using a Nova 2000 series apparatus (Chromatech). The specific surface areas of the materials were calculated using the Brunauer-Emmett-Teller (BET) equation. Prior to the measurements, all the samples were degassed under vacuum at 200 °C for 2 h. Particle sizes were determined from X-ray diffraction (XRD) analysis carried out at room temperature with a Bruker AXS D8 instrument using Cu K_α radiation (λ = 0.1540 nm). The crystallite sizes of composite catalysts were calculated using the Scherrer equation:

$$d = B\lambda/\beta_{1/2}\cos\theta \quad (1)$$

where d is the average particle size of the material under investigation, B is the Scherrer constant (0.89), λ is the wavelength of the X-ray beam, $\beta_{1/2}$ is the full-width at half-maximum of the diffraction peak, and θ is the diffraction angle. The surface morphologies of the prepared catalysts were examined using transmission electron microscopy (TEM; JEOL-JEM-1230) and scanning electron microscopy (SEM; JEOL 5410, Japan). The band-gap energies of the samples were determined by UV-Vis diffuse reflectance spectroscopy (DRS) in air at room temperature in the wavelength range 200–800 nm, using a UV/Vis/NIR spectrophotometer (V-570, JASCO, Japan). The band-gap energies were calculated using the equation

$$E_g = 1239.8/\lambda \quad (2)$$

where E_g is the band gap (eV) and λ is the wavelength of the absorption edges in the spectrum (nm). Photoluminescence (PL) emission spectra were recorded using a fluorescence spectrophotometer (Shimadzu RF-5301). Fourier-transform infrared (FT-IR) spectroscopy was conducted using a Thermo Electron Magna 760 spectrometer. Pellets were made using potassium bromide (KBr, 99% purity, FT-IR grade; Sigma-Aldrich). The catalyst powder was added to the KBr in a mass ratio of 1:100. X-ray photoelectron spectroscopy (XPS) was performed using a SPECS GmbH X-ray photoelectron spectrometer.

2.3. Photocatalyst activity test

The photocatalytic degradation of BBP was conducted in a glass reactor. Visible light was provided by a 300-W Xe lamp with a 400-nm cutoff filter to ensure light irradiation at the desired wavelength. In a typical run, a piece of glass plate coated with a sample film was dipped in 200 ml of aqueous BBP solution (20 mg/L). Prior to the photoreaction, air was pumped into the reaction in the dark for 30 min to achieve adsorption-desorption equilibrium. The light source was then turned on and the BBP solution was continuously pumped during irradiation to maintain the catalyst suspension. The temperature of the suspension was maintained at 30 °C by circulating water through an external cooling jacket and exposing the system to air. At regular intervals, 2 ml of the aqueous solution were collected and centrifuged. The concentration of the remaining BBP was analyzed by high-performance liquid chromatography (HPLC; Waters 2695), performed using a C18 (5 μm) reverse-phase column.

The total organic carbon (TOC) was determined using a Phoenix Total Carbon Analyzer. The degradation intermediates were identified using an Agilent 1100 LC HPLC-mass spectrometry (MS) system, including an electrospray-ionization (ESI) MS, a quaternary pump, a column thermostat, and an automatic sample injector with a 100-μl loop. An Agilent Eclipse XDB-C8 column (4.6 mm × 150 mm), held at 30 °C, was used to separate the intermediate products. The anionic products, i.e., organic acids, were detected using a Dionex ICS2000 ion chromatograph (IC) with a Dionex Ion Pac AS19 analytical column (250 mm × 4 mm i.d.). The mobile phase was 0.8 mmol/L sodium carbonate/1.0 mmol/L sodium bicarbonate, with a flow rate of 1.0 ml/min. The injection volume was 50 μl.

The adsorption capacities of the catalysts were determined using the same method as that used for the photocatalytic activity measurements. The only difference was that the adsorption process was carried out without light irradiation. The results show that BBP adsorption by the thin-film samples after 4 h was approximately zero.

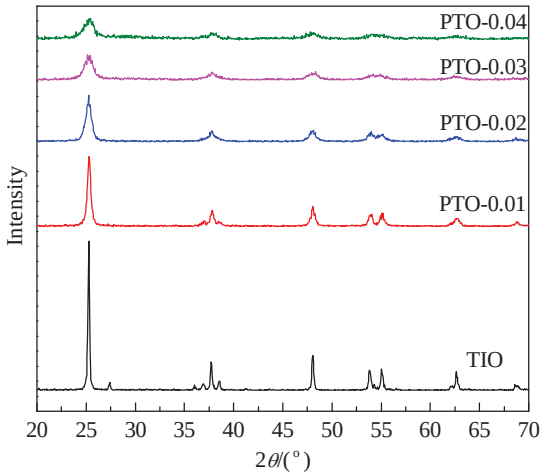

Fig. 1. XRD patterns of TiO_2 and P-doped TiO_2 thin film samples.

3. Results and discussion

3.1. Composite characterization

Figure 1 shows the XRD patterns of TIO, PTIO-0.01, PTIO-0.02, PTIO-0.03, and PTIO-0.04. The patterns show that all the samples consisted of the anatase phase, which demonstrates that the addition of P had no obvious influence on the TiO_2 crystallization process. However, P promoted the crystallization process, because it can be seen from the XRD patterns that the characteristic diffraction peaks of anatase became broader and the diffraction peak intensity decreased. The average crystallite sizes of TiO_2 were calculated form the Scherrer's equation, using the full-width at half-maximum values of the XRD peaks at $2\theta = 25.3°$, corresponding to the most intense anatase peak. The crystallite sizes of TIO, PTIO-0.01, PTIO-0.02, PTIO-0.03, and PTIO-0.04 were 24, 17, 14, 12, and 11 nm, respectively. The particle size therefore became smaller with increasing P concentration.

PL emission spectra have been widely used to investigate the efficiency of charge-carrier trapping, migration, and transfer, and to understand the fate of electron-hole pairs in semiconductor particles [18]. Figure 2 shows the PL spectra of P_{25}, TIO, PTIO-0.01, PTIO-0.02, PTIO-0.03, and PTIO-0.04. The excitonic PL intensities of these samples decrease in the following order: PTIO-0.04 < PTIO-0.03 < PTIO-0.02 < PTIO-0.01 < TIO < P25. This indicates that an appropriate amount of P doping may slow the irradiative recombination of photogenerated electrons and holes in TiO_2, and suggests that the lower the intensity of the PL spectrum, the higher the photocatalytic activity.

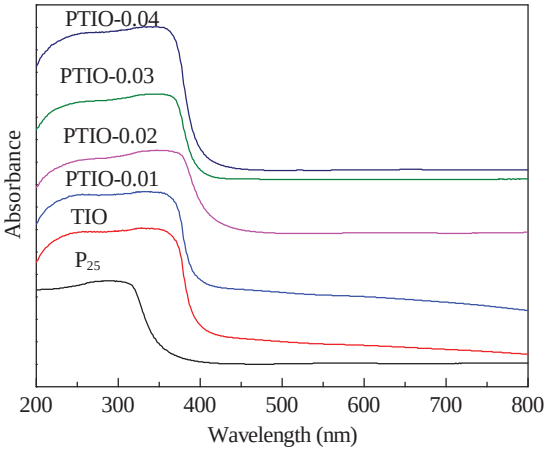

Fig. 3. UV-Vis spectra of P_{25}, TiO_2, and P-doped TiO_2 thin film samples.

The optical absorption properties of a semiconductor, which are related to its electronic structure, are the key factor determining photocatalytic activity. The UV-Vis DRS of P_{25}, TIO, PTIO-0.01, PTIO-0.02, PTIO-0.03, and PTIO-0.04 samples are shown in Fig. 3. The direct band-gap energies for the P_{25}, TIO, PTIO-0.01, PTIO-0.02, PTIO-0.03, and PTIO-0.04 samples, calculated from their reflection spectra, based on a method suggested by Kumar et al. [19], Korosi et al. [20], and Yao et al. [21], are shown in Fig. 4 and tabulated in Table 1. The band gaps of the P_{25} and TIO samples were 3.24 and 3.06 eV, respectively. After doping with P species, the absorption edges of the PTIO samples shifted to the red-light region, and their band gaps were 2.90, 2.80, 2.70, and 2.60 eV for PTIO-0.01, PTIO-0.02, PTIO-0.03, and PTIO-0.0, respectively. The results indicate that the visible-light absorption of the TiO_2 samples was significantly improved by the introduction of P. Therefore,

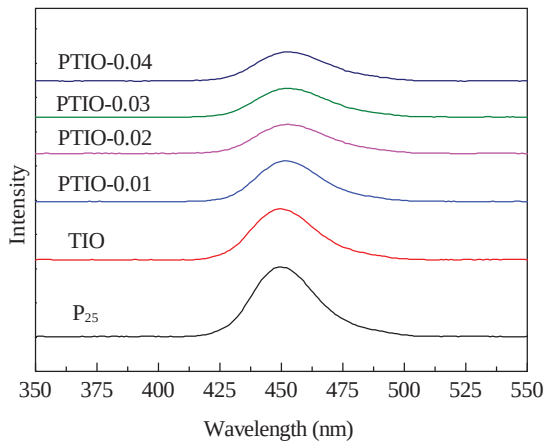

Fig. 2. PL spectra of P_{25}, TiO_2, and P-doped TiO_2 thin film samples.

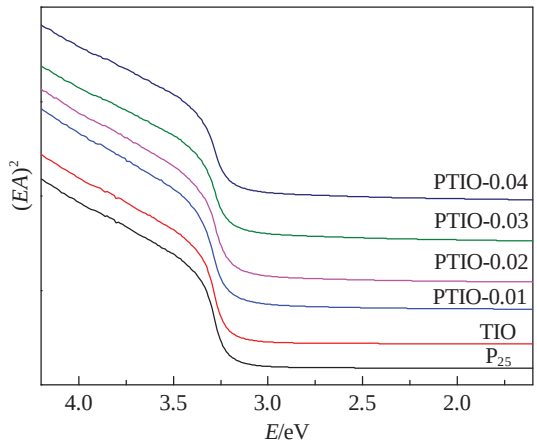

Fig. 4. Band gap of P_{25}, TiO_2, and P-doped TiO_2 thin film samples.

Table 1
BET surface area and band gap of P_{25}, TiO_2, and P-doped samples.

Sample	A_{BET}/(m^2/g)	Band gap (eV)
P25	50	3.24
TIO	70	3.06
PTIO-0.01	100	2.90
PTIO-0.02	130	2.80
PTIO-0.03	140	2.70
PTIO-0.04	155	2.60

the doped samples can be excited by visible light and the photocatalytic activity under visible-light irradiation should be improved.

From Table 1, it can be seen that the BET surface area increased with increasing P concentration. This is because P species inhibit crystal growth, thus significantly enlarging the surface area.

Figure 5 shows the FT-IR spectra of PTIO-0.04 and TIO impregnated with Na_3PO_4 (Na_3PO_4/TiO_2). The results show a broad absorption peak at 1000–1200 cm^{-1}, which is the characteristic frequency region of P–O, in both samples. However, the phosphoryl (P=O) vibration frequencies at 1200–1400 cm^{-1} are absent for PTIO-0.03, implying that the doped P might not simply exist in the form of PO_4^{3-}, but as Ti–O–P. This means that in our preparation, P atoms are incorporated into the TiO_2 lattice.

The chemical forms of the surface elements in the P-doped samples were investigated using XPS analysis. As shown in Fig. 6(a), the XPS peaks in the Ti 2*p* region appear at 458.65 eV (Ti $2p_{3/2}$) and 464.45 eV (Ti $2p_{1/2}$) for PTIO-0.03. The binding energy of Ti $2p_{3/2}$ shifted to a positive value by 0.10 eV compared with that of undoped TiO_2 (458.75 eV). The more electronegative P^{5+} species replace Ti^{4+} species in the surface or near-surface region, pulling the electrons in the Ti–O bond away from the Ti atom, thus causing a small increase in the Ti $2p_{3/2}$ binding energy. The XPS spectrum of P 2*p*, shown in Fig. 6(b), consists of a doublet peak from P $2p_{3/2}$ and P $2p_{1/2}$. The binding energy of P $2p_{3/2}$ in PTIO-0.03 is located at 134.15 eV, indicating the existence of P^{5+}. This value is different from that of P^{5+} in Na_3PO_4-impregnated TiO_2, which is at 133.35 eV. As the ionic radii of Ti^{4+} and P^{5+} are not very similar to each other (0.067 and 0.038 nm, respectively, in an environment with a coordination number of 6), P^{5+} species are unlikely to be present in bulk in high concentrations. We therefore suggest that the doped P may exist in the surface or near-surface region in an octahedral environment, by replacing some of the Ti^{4+}, rather than as PO_4^{3-} in a tetrahedral environment.

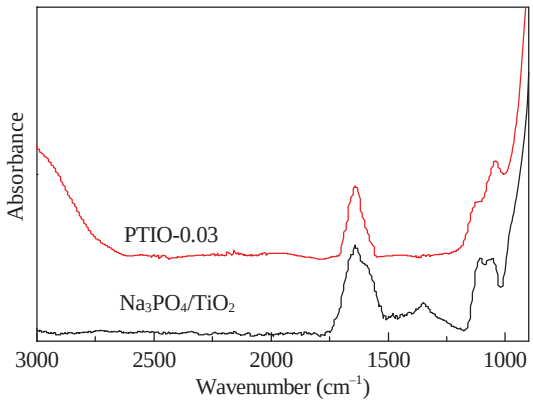

Fig. 5. FT-IR spectra of PTIO-0.03 and Na_3PO_4/TiO_2.

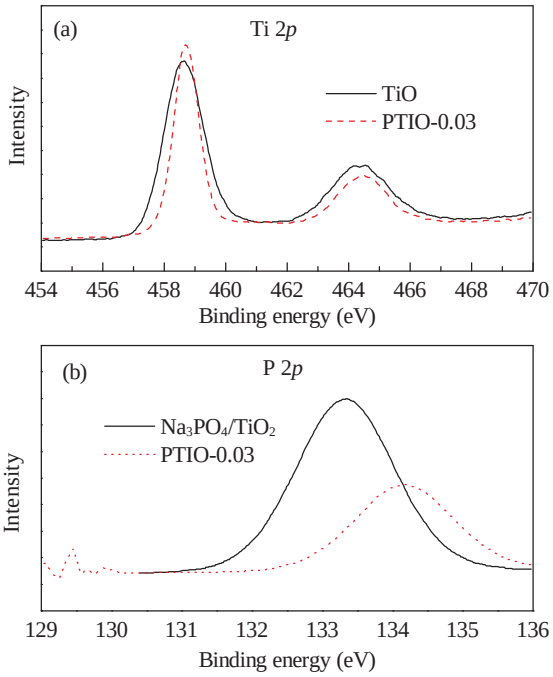

Fig. 6. High resolution XPS spectra of Ti 2*p* for PTIO-0.04 and undoped TIO (a) and P 2*p* for PTIO-0.03 and Na_3PO_4/TiO_2.

The SEM and TEM images of the PTIO-0.03 film are shown in Fig. 7. The SEM image shows that the surface of the PTIO-0.03 film is smooth. The TEM image shows that PTIO-0.03 consists of spherical particles with an average particle diameter of about 11 nm. This is in good agreement with the XRD analysis.

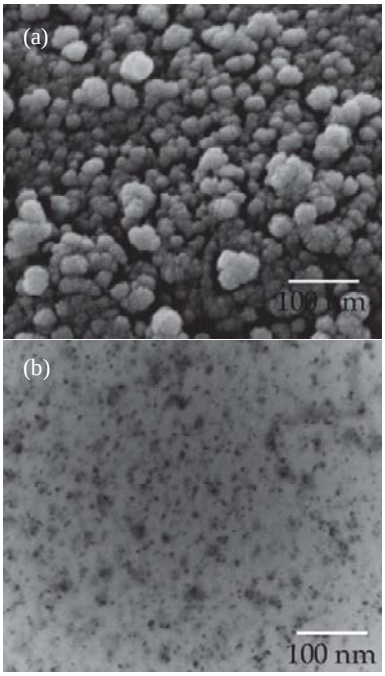

Fig.7. SEM (a) and TEM (b) images of PTIO-0.03.

3.2. Photocatalytic activity

The photocatalytic performances of the PTIO thin-films were investigated using BBP photodegradation. For comparison, an undoped TiO_2 thin-film and P_{25} were also tested under the same conditions. Figure 8 shows the BBP degradation profiles for the different catalysts under visible-light irradiation. No obvious BBP degradation was observed in the absence of a catalyst under visible-light irradiation for 240 min, suggesting that direct photolysis of BBP was negligible. The photodegradation rates of BBP with pure TIO and P_{25} reached only 28% and 17%, respectively. However, more than 98% of the BBP was degraded with the PTIO-0.03 catalyst under the same conditions. The PTIO thin-films are therefore effective visible-light-driven photocatalysts. The contribution of the doped P atoms to the visible-light photocatalytic activity may be achieved by an improvement in the quantum efficiency. The doped P atoms can convert Ti^{4+} to Ti^{3+} via charge compensation. The presence of Ti^{3+} can reduce the electron-hole recombination rate, and further enhance the quantum efficiency and photocatalytic activity [22]. However, the replacement of oxygen in TiO_2 by doped P can cause the absorption edge of TiO_2 to shift to the lower-energy region [23], which can also enhance the photocatalytic activity. The doping of TiO_2 with P atoms therefore results in higher visible-light photocatalytic activity.

The photocatalytic activities of the PTIO samples with various P contents in BBP degradation are shown in Fig. 9. The results show that the photocatalytic activity of the PTIO depends on the P content. The photocatalytic activity increased as the P content increased from 0.01% to 0.03%. At concentrations above 0.03%, however, the photocatalytic activity decreased with increasing P content. The amount of surface Ti^{3+} increases with increasing dopant concentration, so the photocatalytic activities of the PTIOs increased with increasing dopant concentration at low concentrations of dopant. However, new energy levels are formed in the band gap when the amount of surface Ti^{3+} exceeds a certain value [24]. The 3*d* states of Ti^{3+} form defect energy levels of 0–0.35 eV, which are lower than the conduction band, and the new energy levels act as recombination centers [25,26]. So, higher levels of P dopant result in excess surface Ti^{3+} ions, which act as surface recombination centers for electron-hole pairs, and accordingly suppress the photocatalytic activity.

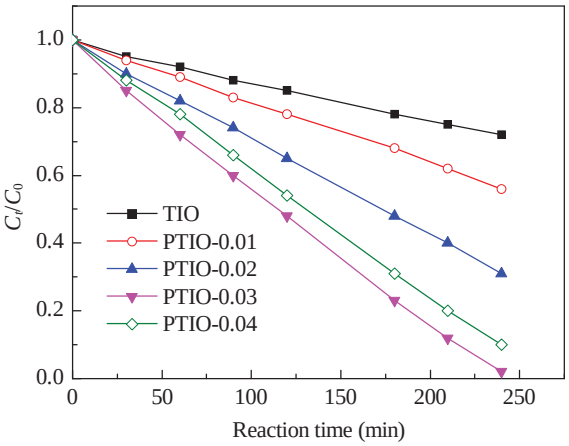

Fig. 9. Photocatalytic activity of the P-doped TiO_2 with various P contents for BBP degradation.

Recycling of catalysts is one of the key factors in assessing the practical applications of photocatalysts and developing heterogeneous photocatalysis technologies for wastewater treatment. An examination of the photocatalytic activity of the recycled PTIO-0.03 catalyst was carried out. The photocatalytic degradation efficiency was 98% during the first six cycles (Fig. 10). The catalytic activity dropped slightly in runs 7, 8, 9, and 10, giving 92%, 88%, 83%, and 78% degradation, respectively. The deactivation of the photocatalyst is probably caused by surface poisoning, which may be induced by adsorbed intermediates. The results show that separation of the photocatalyst is effective, and thus the photocatalyst is basically stable and is promising for use in environmental remediation.

The BBP TOCs, which are determined before and after irradiation of the PTIO-0.03 sample by visible light for 240 min, are 640 and 14, respectively. The results show that the BBP percentage removal efficiency was 97.8%, which is in close agreement with the results obtained using HPLC (98%), and confirm that all the decomposed BBP was degraded to carbon dioxide.

To investigate the BBP photodegradation pathway, some of the degradation intermediates were tentatively identified using

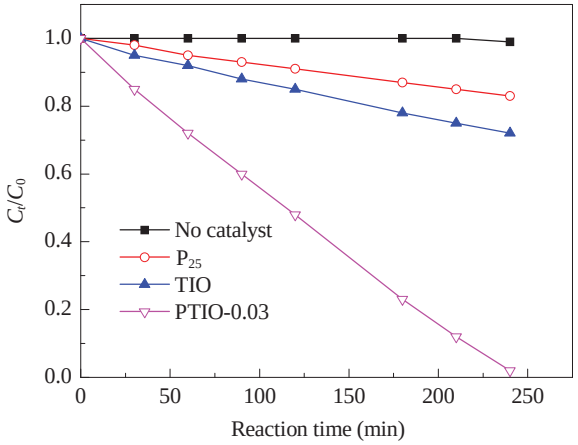

Fig. 8. Photocatalytic activity of different catalysts for BBP degradation under visible light irradiation.

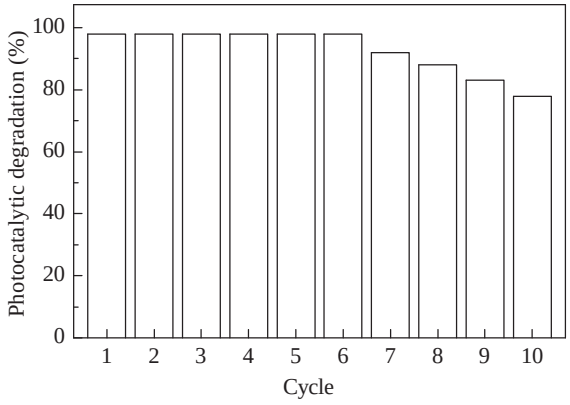

Fig. 10. Recycle and reuse of photocatalysts for BBP photocatalytic degradation.

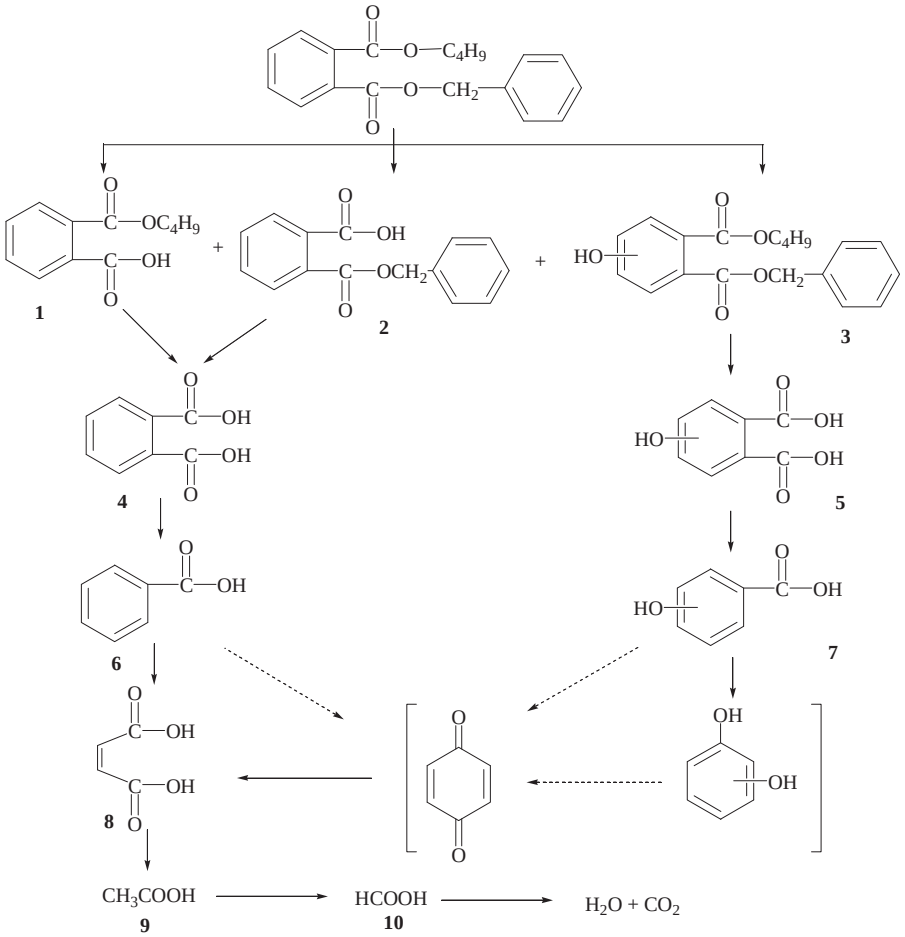

Scheme 1. Proposed degradation pathway of BBP under visible light irradiation by using P-TiO_2 thin film.

HPLC-MS and IC. Compounds **1**–**7** (Scheme 1) were identified using ESI-MS, and maleic acid, acetic acid, and formic acid were identified using IC. The proposed photocatalytic degradation pathway of BBP catalyzed by PTIO under visible-light irradiation, based on the identified intermediate products and literature reports [27–29], is presented in Scheme 1. The first step was an electron-transfer reaction, involving attack by •OH radicals. There are two possible positions for attack by •OH radicals: the carbonyl group and the aromatic ring of the BBP molecule. Compounds **1** and **2** were generated by cleavage of the alkyl-oxygen bond of BBP when •OH radicals attacked the carbonyl group. The attack by •OH radicals of the aromatic ring led to the formation of hydroxylated intermediate isomers (compound 3). Compounds **1**–**3** were further attacked by •OH radicals, forming compounds **4** and **5**. Decarboxylation of compounds **4** and **5** resulted in compounds **6** and **7**. Further decarboxylation of compounds **6** and **7** led to dihydroxybenzene and quinone. Quinone was further oxidized, resulting in a series of aliphatic acids, including maleic acid, acetic acid, and formic acid. These aliphatic acids were then further oxidized to produce carbon dioxide and water.

4. Conclusions

PTIO thin-film photocatalysts were successfully prepared using a sol-gel method. The PTIO composites generated were nanosized, relatively uniform, and homogeneously dispersed. The addition of P played a promoting role in the crystallization process, and prevented agglomeration during calcination. The PTIO photocatalysts were effective in BBP photocatalytic degradation under visible-light irradiation. The high photocatalytic activities of the PTIO thin-films may be the result of extrinsic absorption through the creation of oxygen vacancies, rather than extrinsic absorption by bulk TiO_2. Catalyst re-use results showed that the present photocatalysts remain effective and active after six cycles, indicating promising recyclability of the PTIO photocatalysts.

References

[1] Keith L, Telliard W. *Environ Sci Technol*, 1979, 13: 416
[2] Yu H, Hu J Y, Jin X H, He W J, Han H D. *Water Wastewater Eng*, 2005, 31: 20
[3] Xu L, Yang X, Guo Y H, Ma F Y, Guo Y N, Yuan X, Huo M X. *J Hazard Mater*, 2010, 178: 1070
[4] Ding X J, An T C, Li G Y, Chen J X, Sheng G Y, Fu J M, Zhao J C. *Res Chem Intermed*, 2008, 34: 67
[5] Zhao X K, Yang G P, Wang Y J, Gao X C. *J Photochem Photobiol A*, 2004, 161: 215
[6] Chiou C S, Shie J L, Chang C Y, Liu C C, Chan C T. *J Hazard Mater*, 2006, 137: 1123

Graphical Abstract

Chin. J. Catal., 2013, 34: 1267–1273 doi: 10.1016/S1872-2067(12)60572-5

Synthesis and characterization of P-doped TiO_2 thin-films for photocatalytic degradation of butyl benzyl phthalate under visible-light irradiation

R. M. MOHAMED *, E. AAZAM
King Abdulaziz University, Saudi Arabia;
Central Metallurgical R&D Institute, Egypt

P-doped TiO_2 thin-film photocatalysts can degrade waste materials under visible-light irradiation.

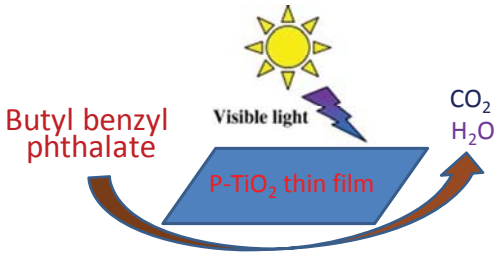

[7] Kaneco S, Katsumata H, Suzuki T, Ohta K. *Chem Eng J*, 2006, 125: 59
[8] Asahi R, Morikawa T, Ohwaki T, Aoki K, Taga Y. *Science*, 2001, 293: 269
[9] Senthilnathan J, Philip L. *Chem Eng J*, 2011, 172: 678
[10] Bianchi C L, Cappelletti G, Ardizzone S, Gialanella S, Naldoni A, Oliva C, Pirola C. *Catal Today*, 2009, 144: 31
[11] Gorska P, Zaleska A, Hupka J. *Sep Purif Technol*, 2009, 68: 90
[12] Irie H, Watanabe Y, Hashimoto K. *Chem Lett*, 2003, 32: 772
[13] Xu J J, Ao Y H, Chen M D. *Mater Lett*, 2009, 63: 2442
[14] Zaleska A, Sobczak J W, Grabowska E, Hupka J. *Appl Catal B*, 2008, 78:
[15] Wang Y P, Li J, Peng P Y, Lu T H, Wang L J. *Appl Surf Sci*, 2008, 254: 5276
[16] Tian H, Ma J F, Li K, Li J J. *Ceram Int*, 2009, 3: 1289
[17] Xu L, Tang C Q, Qian J, Huang Z B. *Appl Surf Sci*, 2010, 256: 2668
[18] Yamashita H, Ichihashi Y, Zhang S G, Matsumura Y, Souma Y, Tatsumi T, Anpo M. *Appl Surf Sci*, 1997, 121: 305
[19] Kumar V, Sharma S Kr, Sharma T P. *Opt Mater*, 1999, 12: 115
[20] Korosi L, Dekany I. *Colloids Surf A*, 2006, 280: 146
[21] Yao S H, Jia X Y, Jiao L L, Zhu C, Shi Z L. *Indian J Chem*, 2012, 51: 1049
[22] Yu J C, Yu J G, Ho W K, Jiang Z T, Zhang L Z. *Chem Mater*, 2002, 12: 3808
[23] Luo H M, Takata T, Lee Y, Zhao J F, Domen K, Yan Y S. *Chem Mater*, 2004, 16: 846
[24] Takeda S, Suzuki S, Odaka H, Hosono H. *Thin Solid Films*, 2001, 392: 338
[25] Wang J, Tafen D N, Lewis J P, Hong Z L, Manivannan A, Zhi M J, Li M, Wu N Q. *J Am Chem Soc*, 2009, 131: 12290
[26] Ikeda S, Sugiyama N, Murakami S, Kominami H, Kera Y, Noguchi H, Uosaki K, Torimoto T, Ohtani B. *Phys Chem Chem Phys*, 2003, 5: 778
[27] Xu L, Yang X, Guo Y H, Ma F Y, Guo Y N, Yuan X, Huo M X. *J Hazard Mater*, 2010, 178: 1070
[28] Ning F X, Lu Y, Zhang T Y. *Chin J Environ Chem*, 2006, 25: 567
[29] Xu X R, Li S X, Li X Y, Gu J D, Chen F, Li X Z, Li H B. *J Hazard Mater*, 2009, 164: 527